



**HAL**  
open science

# WGMode: A Matlab toolbox for whispering gallery modes volume computation in spherical optical micro-resonators

Stéphane Balac

► **To cite this version:**

Stéphane Balac. WGMode: A Matlab toolbox for whispering gallery modes volume computation in spherical optical micro-resonators. *Computer Physics Communications*, 2019, 243, pp.121-134. 10.1016/j.cpc.2019.05.002 . hal-02129778

**HAL Id: hal-02129778**

**<https://hal.science/hal-02129778>**

Submitted on 15 May 2019

**HAL** is a multi-disciplinary open access archive for the deposit and dissemination of scientific research documents, whether they are published or not. The documents may come from teaching and research institutions in France or abroad, or from public or private research centers.

L'archive ouverte pluridisciplinaire **HAL**, est destinée au dépôt et à la diffusion de documents scientifiques de niveau recherche, publiés ou non, émanant des établissements d'enseignement et de recherche français ou étrangers, des laboratoires publics ou privés.

# WGMode : A Matlab toolbox for whispering gallery modes volume computation in spherical optical micro-resonators

Stéphane Balac\*

UNIV RENNES, CNRS, IRMAR - UMR 6625, F-35000 Rennes, France

---

## Abstract

We present a MATLAB toolbox aimed at studying Whispering Gallery Modes (WGM) in spherical optical micro-resonators. Whispering gallery modes are specific resonances of an optical wave trapped inside a dielectric cavity with smooth edges due to continuous total internal reflection of light. The novelty of the work stands in the implementation of analytical formulas to compute the volume of a WGM in a spherical cavity while only approximate asymptotic expressions or purely numerical computations based on the Finite Element Method were previously available. The toolbox also provides MATLAB programs to compute and visualize WGM.

*Keywords:* optical micro-resonators, whispering gallery modes, mode volume

---

## PROGRAM SUMMARY

*Program Title:* WGMODE

*Licensing provisions:* LGPL

*Programming language:* MATLAB language

### *Nature of problem:*

The WGMODE toolbox has been developed to compute the volume of a Whispering Gallery Mode (WGM) in a spherical optical micro-resonator [1]. The volume of a WGM is defined as the integral over the whole space of the energy density normalized by its maximum value [2]. Together with the quality factor, the mode volume is used to characterize WGM. The WGMODE toolbox gathers together several MATLAB scripts aimed at studying WGM in a spherical optical micro-resonator.

### *Solution method:*

The volume of a WGM is defined as the integral over the whole space of the energy density normalized by its maximum value. For a spherical dielectric cavity, an analytical expression of the electromagnetic field for a WGM can be computed analytically

---

\*Corresponding author.

*E-mail address:* stephane.balac@univ-rennes1.fr

from Maxwell's equations using Hansen's method [2]. The expression of the mode field involves Vector Spherical Harmonics and requires the finding of roots of a non-linear equation with Bessel's functions. From the analytical expression of the mode field, the mode volume integral can be computed analytically. These formulas are implemented in the WGMODE toolbox to compute the volume of a WGM.

*Additional comments including Restrictions and Unusual features:*

The WGMODE toolbox has been tested with MATLAB version 8.1 (R2013a), version 9 (R2016a), version 9.4 (R2018a). The WGMODE toolbox also works under GNU OCTAVE software (tested with version 4.0.0). However, under GNU OCTAVE the scripts `pltmod` and `volmod` written to display the mode field (electric field and magnetic induction parts) and to compute the mode volume provide the results after an excessive time due to the computation of the Vector Spherical Harmonics that is not efficient under OCTAVE.

## References

- [1] J. Ward, O. Benson, WGM micro-resonators: sensing, lasing and fundamental optics with microspheres, *Laser & Photonics Reviews* 5 (4) (2011) 553–570.
- [2] A. N. Oraevsky, Whispering-gallery waves, *Quantum Electronics* 32 (2002) 377–400.

## 1. Introduction

Optical Whispering gallery modes (WGM) are specific resonances of electromagnetic waves inside a dielectric cavity (the resonator) with smooth surface. They correspond to light-waves circling around the cavity, almost perfectly guided round by optical total internal reflection, that meet a resonance condition (after one round-trip they return to the same point with the same phase and hence interfere constructively with themselves, forming standing waves). The unique combination of strong temporal and spatial confinement of light in an optical micro-resonator makes these systems of interest for various applications in optics such as lasing, frequency comb generation, sensing, *etc.* For a review on micro-resonators' fundamentals, fabrication processes and applications, we refer to [1, 2, 3, 4].

Among the various shapes for the dielectric cavity (disks, rings, toroids, photonic crystal cavities, cylindrical optical fibers, *etc.*), although less easily integrable, spherical micro-resonators have the advantage of being the simplest three-dimensional WGM resonator and they can exhibit very high quality factors. Spherical micro-resonators are typically ten to hundred micrometers in diameter, and they are often fabricated in silica glass by simply melting the tip of a conventional single-mode fiber [2, 3, 4, 5].

Properties of WGM in an optical microcavity are well described by the quality factor  $Q$  of the mode that accounts for energy losses and is related to the temporal confinement of light and by its mode volume  $\mathcal{V}$  that accounts for spatial

confinement of light. Depending on the shape of the dielectric cavity, numerical computation of these two quantities can be complicated. Spherical cavity is the only rare exception.

A part of optical losses in an optical micro-resonator is caused by the fact that, unlike a flat surface, the total internal reflection from a curved surface does not exist and leads to a radiation of the wave from the dielectric cavity [5, 6, 7]. This phenomenon is taken into account through the *radiative quality factor* which is defined as the ratio of the real part of the wave number of a given WGM and its imaginary part. Other energy losses in a micro-resonator include surface scattering losses, surface absorption losses, material absorption losses and are taken into account in the definition of the *intrinsic quality factor*. These additional contributions to the quality factor are difficult to handle mathematically and to compute analytically [6, 7, 8]. For this reason, in the WGMODE toolbox only the radiative quality factor is computed.

The WGMODE toolbox was primarily written to compute the mode volume  $\mathcal{V}$  of a WGM in a spherical micro-resonator. The mode volume is defined as the ratio of the total energy stored inside the resonator for that mode and the maximum energy density of the mode [9, Sec. 1.6], [10, Sec. 2.7]:

$$\mathcal{V} = \frac{1}{M} \iiint_{\mathbb{R}^3} \left( \frac{\varepsilon(\mathbf{r})}{2} \|\mathbf{E}(\mathbf{r})\|^2 + \frac{1}{2\mu(\mathbf{r})} \|\mathbf{B}(\mathbf{r})\|^2 \right) d\mathbf{r} \quad (1)$$

where  $\mathbf{E}$  and  $\mathbf{B}$  are respectively the electric field and magnetic induction of the mode,  $\mu$  and  $\varepsilon$  are respectively the magnetic permeability and electric permittivity,  $M = \max_{\mathbf{r} \in \mathbb{R}^3} \left( \frac{\varepsilon(\mathbf{r})}{2} \|\mathbf{E}(\mathbf{r})\|^2 + \frac{1}{2\mu(\mathbf{r})} \|\mathbf{B}(\mathbf{r})\|^2 \right)$  is the maximum of the energy density of the optical mode and  $\|\cdot\|$  denotes the euclidean norm in  $\mathbb{C}^3$ . Note that the definition (1) of the mode volume is open to question since integrating over the entire space leads to a diverging integral since modes of an optical micro-resonator grow exponentially at infinity (see below the expression (3)–(4) of a TE mode). This issue is mostly ignored in the literature and overcome by integrating over a finite integration domain. Such an approach can result in relatively small errors when dealing with modes of high quality factor. We refer to [11] for a detailed discussion of the issue and nevertheless we adopt formula (1) as expression of the mode volume. Mode volume provides relevant information on WGM features. It is related to the free spectral range (FSR): lower mode volume means higher FSR. For lasing applications of micro-resonators it is also related to the lasing characteristics since stimulated as well as spontaneous emission rates are inversely proportional to the mode volume whereas the lasing threshold is directly proportional to the mode volume [12]. For sensing applications of micro-resonators, the mode volume is a parameter connected with the coupling of the resonator and related to its sensitivity to external parameters [13].

The novelty of the WGMODE toolbox is to provide tools to compute the volume of a WGM in a spherical optical micro-resonator based on an analytical approach to evaluate the volume integral in (1). This ensures both accurate results and fast computation times. Alternative approaches investigated in the

literature to compute the volume of a WGM include approximate formulas based on asymptotic expansions of the mode field [9, 10, 8] and purely numerical computations based on the Finite Element Method (FEM) [14, 15]. The advantage of mode volume formulas based on asymptotic expansions of the WGM field is their simplicity. However, they are based on strong assumptions that limit their domain of validity to a restricted range of possible values for the mode indexes and geometric size of the cavity. Opposite is the use of the FEM to compute the WGM field and mode volume. The FEM does not introduce geometric limitations or assumptions on the mode indexes of the WGM. However, computation can take a long time compared to the use of analytical formulas, but more importantly it is not at all obvious to determine the mode indexes of the WGM from a FEM computation which can be considered as a severe disadvantage for the study of spherical optical micro-resonators.

The paper is organized as follows. In section 2, we recall the expression of WGM field in a spherical optical micro-resonator as it can be found e.g. in [8, 5]. In section 3, we show how the mode volume integral (1) can be computed analytically starting from the expression of the WGM field given in Section 2. Section 4 is devoted to an overview of the WGMODE toolbox, including a comprehensive test run. Finally, we conclude in Section 5 by presenting benchmark results comparing the three approaches mentioned above for computing the mode volume of a WGM in a spherical micro-resonator.

## 2. Expression of WGM in a spherical micro-resonator

For a spherical dielectric cavity, an analytical expression of the electromagnetic field

$$\mathbf{E}(\mathbf{r}, t) = \text{Re}[\underline{\mathbf{E}}(\mathbf{r}) \exp(i\omega t)], \quad \mathbf{B}(\mathbf{r}, t) = \text{Re}[\underline{\mathbf{B}}(\mathbf{r}) \exp(i\omega t)] \quad (2)$$

corresponding to a WGM ( $\omega$  denotes the resonance frequency) is obtained from Maxwell's harmonic equations using the so-called Hansen's method [16]. We denote by  $N$  the optical index of the dielectric cavity and by  $R$  its radius. We set  $k_0 = \omega/c$  and  $k = k_0 N$ . Using Hansen's method, it is found that there exist two kinds of electromagnetic fields with different polarization termed TE (transverse electric) and TM (transverse magnetic) defined in spherical coordinates  $(r, \theta, \varphi)$ , see Fig. 1, as follows [8, 5]. For TE modes, the mode field can be expressed as

$$\underline{\mathbf{E}}(r, \theta, \varphi) = \begin{cases} \frac{\psi_\ell(kr)}{kr} \mathbf{X}_{\ell m}(\theta, \varphi) & \text{if } r \leq R \\ \frac{k_0}{k} \frac{\psi_\ell(kR)}{\zeta_\ell(k_0 R)} \frac{\zeta_\ell(k_0 r)}{k_0 r} \mathbf{X}_{\ell m}(\theta, \varphi) & \text{if } r > R \end{cases} \quad (3)$$

and

$$\underline{\mathbf{B}}(r, \theta, \varphi) = \begin{cases} \frac{ik}{\omega} \left( \ell(\ell+1) \frac{\psi_\ell(kr)}{k^2 r^2} \mathbf{Z}_{\ell m}(\theta, \varphi) \right. \\ \quad \left. + \frac{\psi'_\ell(kr)}{kr} \mathbf{Y}_{\ell m}(\theta, \varphi) \right) & \text{if } r \leq R \\ \frac{ik_0^2}{k\omega} \frac{\psi_\ell(kR)}{\zeta_\ell(k_0 R)} \left( \ell(\ell+1) \frac{\zeta_\ell(k_0 r)}{k_0^2 r^2} \mathbf{Z}_{\ell m}(\theta, \varphi) \right. \\ \quad \left. + \frac{\zeta'_\ell(k_0 r)}{k_0 r} \mathbf{Y}_{\ell m}(\theta, \varphi) \right) & \text{if } r > R \end{cases} \quad (4)$$

where  $\ell, m$  are integers such that  $-\ell \leq m \leq \ell$ ,  $\mathbf{X}_{\ell m}$ ,  $\mathbf{Y}_{\ell m}$  and  $\mathbf{Z}_{\ell m}$  denote the *Vector Spherical Harmonics* defined from the *Scalar Spherical Harmonics*  $Y_\ell^m$  as

$$\mathbf{Z}_{\ell m} = Y_\ell^m \mathbf{e}_r, \quad \mathbf{Y}_{\ell m} = r \nabla Y_\ell^m, \quad \mathbf{X}_{\ell m} = \nabla Y_\ell^m \wedge \mathbf{r} \quad (5)$$

and  $\psi_\ell$  and  $\zeta_\ell$  denote respectively the *Riccati-Bessel functions* of first and third kinds. They are related to the Bessel function  $J_{\ell+\frac{1}{2}}$  and Hankel function  $H_{\ell+\frac{1}{2}}^{(2)}$  respectively by [17, 18]

$$\psi_\ell(x) = \sqrt{\frac{\pi x}{2}} J_{\ell+\frac{1}{2}}(x), \quad \zeta_\ell(x) = \sqrt{\frac{\pi x}{2}} H_{\ell+\frac{1}{2}}^{(2)}(x). \quad (6)$$

The Spherical Surface Harmonics of degree  $\ell$  and order  $m$  is defined as, see [19],

$$Y_\ell^m(\theta, \varphi) = C_{\ell m} P_\ell^m(\cos(\theta)) e^{im\varphi} \quad -\ell \leq m \leq \ell, \quad \ell \in \mathbb{N} \quad (7)$$

where the normalization constant  $C_{\ell m}$  is taken to be

$$C_{\ell m} = \sqrt{\frac{(2\ell+1)(\ell-m)!}{4\pi(\ell+m)!}}. \quad (8)$$

Note that the mode field  $(\underline{\mathbf{E}}, \underline{\mathbf{B}})$  given by (3)–(4) is defined up to a normalization constant. Note also that Hankel function  $H_{\ell+\frac{1}{2}}^{(2)}$ , and its Riccati-Bessel counterpart  $\zeta_\ell$  used in (3)–(4), express outward-propagating spherical-wave solutions of the spherical wave equation for the sign convention  $+i\omega t$  used here for the frequency in (2).

For TM modes, we have

$$\underline{\mathbf{E}}(r, \theta, \varphi) = \begin{cases} \ell(\ell+1) \frac{\psi_\ell(kr)}{k^2 r^2} \mathbf{Z}_{\ell m}(\theta, \varphi) + \frac{\psi'_\ell(kr)}{kr} \mathbf{Y}_{\ell m}(\theta, \varphi) & \text{if } r < R \\ \frac{\psi_\ell(kR)}{\zeta_\ell(k_0 R)} \left( \ell(\ell+1) \frac{\zeta_\ell(k_0 r)}{k_0^2 r^2} \mathbf{Z}_{\ell m}(\theta, \varphi) \right. \\ \quad \left. + \frac{\zeta'_\ell(k_0 r)}{k_0 r} \mathbf{Y}_{\ell m}(\theta, \varphi) \right) & \text{if } r > R \end{cases} \quad (9)$$

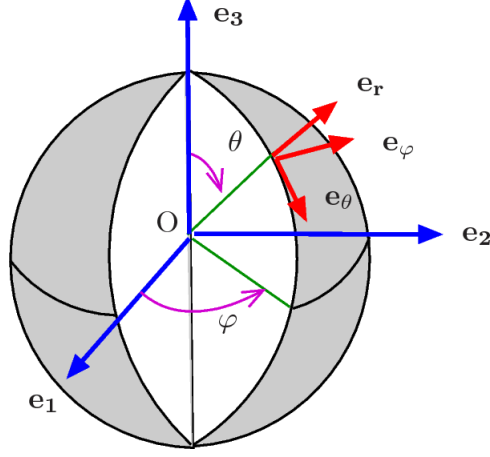


Figure 1: Definition of the spherical coordinate system used.

and

$$\underline{\mathbf{B}}(r, \theta, \varphi) = \begin{cases} \frac{ik}{\omega} \frac{\psi_\ell(kr)}{kr} \mathbf{X}_{\ell m}(\theta, \varphi) & \text{if } r \leq R \\ \frac{ik_0}{\omega} \frac{\psi_\ell(kR)}{\zeta_\ell(k_0R)} \frac{\zeta_\ell(k_0r)}{k_0r} \mathbf{X}_{\ell m}(\theta, \varphi) & \text{if } r > R \end{cases} \quad (10)$$

Here again, the mode field ( $\underline{\mathbf{E}}, \underline{\mathbf{B}}$ ) given by (9)–(10) is defined up to a normalization constant.

Resonance frequencies  $\omega$  are obtained by solving the so-called *modal equation* [8, 5]

$$P \frac{\psi'_\ell(kR)}{\psi_\ell(kR)} = \frac{\zeta'_\ell(k_0R)}{\zeta_\ell(k_0R)} \quad (11)$$

where  $P = N$  for TE modes and  $P = 1/N$  for TM modes. As a consequence, a mode is described in terms of three integers: the integer  $\ell$  involved in the modal equation (11), one integer  $n$  used to label the solutions of the modal equation (11) for a fixed value of  $\ell$  and the integer  $m$  involved in the expression of the electromagnetic field of the mode, see (3)–(4) and (9)–(10). Note that this underscores a mode degeneracy since there exist  $2\ell + 1$  modes with the same values of  $\ell$  and  $n$ , and therefore with the same resonance frequency  $\omega$ , but with a different value for  $m$  and therefore with a different expression for the electromagnetic field. It can be shown that the *polar mode number*  $\ell$  is equal to the number of wavelengths taken to travel around the sphere and that the *radial mode number*  $n$  is equal to the number of intensity maxima of the mode in the radial direction  $\mathbf{e}_r$ . The index  $m$  is called the *azimuthal mode number*. It can take  $2\ell + 1$  values from  $-\ell$  to  $\ell$  and it is related to the sinusoidal variation of the mode with the azimuthal angle  $\varphi$ . Negative values of  $m$  signify counter-propagating modes. Moreover,  $\ell - |m| + 1$  is the number of intensity

maxima in the polar direction  $\mathbf{e}_\theta$ . Thus modes with index  $n = 1$  correspond to the best confined modes in the radial direction and modes for which  $m = \ell$  are the best confined in the polar direction. The mode satisfying these conditions, and corresponding to the highest value of  $\ell$  for which the modal equation (11) has a solution, is termed the *fundamental mode*. WGM refers in the literature to modes with polar index  $\ell$  close to the highest possible value for which the modal equation (11) has a solution, together with a small difference  $\ell - |m|$  and  $n$  close to unity [8].

Frequencies  $\omega$  obtained as solutions to the modal equation (11) are complex valued. It is usual in the study of WGM in optical micro-resonators to introduce the *radiative quality factor* as the ratio of the real part of the resonance frequency  $\omega$  and its imaginary part:

$$Q = \frac{\text{Re}(\omega)}{\text{Im}(\omega)}. \quad (12)$$

The smaller losses by radiation are, the smaller  $\text{Im}(\omega)$  is and therefore the higher is the radiative quality factor. We wish to emphasize that the quality factor of an optical micro-resonator usually takes into account other losses phenomena, that can be predominant [6, 7, 8]. Therefore, it is likely to happen that the radiative quality factor is not close to the true, experimentally measured, quality factor.

In practice, spherical optical micro-resonators often correspond to resonators with a large radius compared to the resonance wavelength  $\lambda = \omega/c$  of interest in the optical domain. For such resonators, the solutions to the modal equation (11) corresponding to WGM are related to large values of the polar mode index  $\ell$ . For example, if we consider a  $50 \mu\text{m}$  radius silica sphere at a wavelength  $\lambda \approx 1.5 \mu\text{m}$ , we obtain the highest values of  $\ell$  greater than 300, see Section 4. As a consequence, for such a mode the radiative leakage of the energy is small and a good approximation consists in assuming the radiative part outside the sphere as negligible. From a mathematical point of view, this approximation consists in considering the following asymptotic expansions of Bessel's functions for large order  $\ell$ , see e.g. [17, formula 10.19.2]:  $\zeta_\ell(z) \approx i\chi_\ell(z)$  where  $\chi_\ell$  denotes Riccati-Bessel function of the second kind with order  $\ell$  related to Bessel function  $Y_{\ell+\frac{1}{2}}$  by

$$\chi_\ell(x) = -\sqrt{\frac{\pi x}{2}} Y_{\ell+\frac{1}{2}}(x). \quad (13)$$

Analytical formulas for modes volume in spherical optical micro-resonators presented in the next section and implemented in the WGMODE toolbox were obtained under this assumption, mathematically restrictive but very realistic from a practical viewpoint. This approximation leads to consider the following form for the modal equation

$$P \frac{\psi'_\ell(kR)}{\psi_\ell(kR)} = \frac{\chi'_\ell(k_0R)}{\chi_\ell(k_0R)} \quad (14)$$

that admits real solution  $k_0$ .

### 3. Computation of the volume of a whispering gallery mode

The volume of a whispering gallery mode is mathematically defined by formula (1). Here we make the assumption that the dielectric cavity is non-magnetic, *i.e.* its magnetic permeability  $\mu$  is the one of vacuum ( $\mu = \mu_0$ ). When we assume that the energy losses by diffraction and diffusion can be neglected, the energy conservation law implies that the contribution of the electric field and the magnetic field to the energy density is equal [20]:

$$\iiint_{\mathbb{R}^3} \frac{\varepsilon(\mathbf{r})}{2} \|\mathbf{E}(\mathbf{r})\|^2 \, d\mathbf{r} = \iiint_{\mathbb{R}^3} \frac{1}{2\mu_0} \|\mathbf{B}(\mathbf{r})\|^2 \, d\mathbf{r}. \quad (15)$$

As a consequence, the volume of a WGM is most often computed in the literature [9, 10, 4, 8, 15] from the following formula:

$$\mathcal{V} = \frac{1}{\varepsilon_0 N^2 E_{\max}^2} \iiint_{\mathbb{R}^3} \varepsilon(\mathbf{r}) \|\mathbf{E}(\mathbf{r})\|^2 \, d\mathbf{r} \quad (16)$$

where  $E_{\max}$  denotes the maximum value of the Euclidean norm of the electric field. Formula (16) is well suited for the computation of the mode volume of a TE mode in a spherical optical micro-resonator because of the simple expression of the electric field for TE mode, see (3). It should be noted however that the normalization constant is not the same in (1) and in (16).

For TM modes the mathematical expression of the electric field given by (9) is much complicated than for TE modes. That is why computation of the mode volume from (16) is not recommended. It is much preferable to use relation (15) to express the volume of a TM mode as

$$\mathcal{V} = \frac{c^2}{N^2 E_{\max}^2} \iiint_{\mathbb{R}^3} \|\mathbf{B}(\mathbf{r})\|^2 \, d\mathbf{r} \quad (17)$$

where  $c$  is the speed of light in free space. Unfortunately, the normalization constant in (16) can't be expressed in terms of  $\mathbf{B}$  and changing it for  $\max_{\mathbf{r} \in \mathbb{R}^3} \|\mathbf{B}(\mathbf{r})\|^2$  would not be consistent when comparing volumes of TE and TM modes.

#### 3.1. Volume of a TE mode

Because of the evanescent behavior of the electromagnetic field outside the micro-sphere for WGM, we bound the integration domain in (16) at a radial distance  $L > R$  appropriately selected. For TE modes, the mode volume is therefore given in spherical coordinates as

$$\mathcal{V} = \frac{1}{\varepsilon_0 N^2} \int_0^L \int_0^\pi \int_0^{2\pi} \varepsilon(r) \frac{\|\mathbf{E}(r, \varphi, \theta)\|^2}{E_{\max}^2} r^2 \sin(\theta) \, d\varphi d\theta dr. \quad (18)$$

For TE modes, given the approximation of the mode field outside the sphere discussed in p. 7, the electric field is given in spherical coordinates by

$$\underline{\mathbf{E}}(r, \theta, \varphi) = \begin{cases} \frac{\psi_\ell(kr)}{kr} \mathbf{X}_{\ell m}(\theta, \varphi) & \text{for } 0 \leq r \leq R \\ \frac{\psi_\ell(kR)}{\chi_\ell(k_0 R)} \frac{\chi_\ell(k_0 r)}{k_0 r} \mathbf{X}_{\ell m}(\theta, \varphi) & \text{for } R < r \leq L \end{cases} \quad (19)$$

Using Chasles's theorem, we split the integral in (18) into two parts such that the first integral corresponds to the part  $\mathcal{V}_i$  of the mode volume over the cavity and the second integral to the part  $\mathcal{V}_o$  of the mode volume over the exterior domain:  $\mathcal{V} = \mathcal{V}_i + \mathcal{V}_o$ . We have

$$\begin{aligned}\mathcal{V}_i &= \frac{1}{k^2 E_{\max}^2} \int_0^R \int_0^\pi \int_0^{2\pi} \psi_\ell^2(kr) \|\mathbf{X}_{\ell m}(\varphi, \theta)\|^2 \sin(\theta) \, d\varphi d\theta dr \\ &= \frac{1}{k^2 E_{\max}^2} \left( \int_0^R \psi_\ell^2(kr) \, dr \right) \left( \int_0^\pi \int_0^{2\pi} \|\mathbf{X}_{\ell m}(\varphi, \theta)\|^2 \sin(\theta) \, d\varphi d\theta \right).\end{aligned}\quad (20)$$

As a consequence of the orthogonality properties of Vector Spherical Harmonics, we have

$$\int_0^\pi \int_0^{2\pi} \|\mathbf{X}_{\ell m}(\varphi, \theta)\|^2 \sin(\theta) \, d\varphi d\theta = \ell(\ell + 1).\quad (21)$$

Therefore,

$$\mathcal{V}_i = \frac{\ell(\ell + 1)}{k^2} \frac{1}{E_{\max}^2} \int_0^R \psi_\ell^2(kr) \, dr = \frac{\ell(\ell + 1)}{k} \frac{1}{E_{\max}^2} \frac{\pi}{2} \int_0^R r J_{\ell+\frac{1}{2}}^2(kr) \, dr.$$

This last integral can be calculated thanks to [21, formula 5.54 p. 629]

$$\int x J_p(\alpha x)^2 \, dx = \frac{x^2}{2} (J_p(\alpha x)^2 - J_{p-1}(\alpha x) J_{p+1}(\alpha x)).$$

We obtain

$$\mathcal{V}_i = \frac{\ell(\ell + 1)\pi R^2}{4k} \frac{1}{E_{\max}^2} \left( J_{\ell+\frac{1}{2}}^2(kR) - J_{\ell-\frac{1}{2}}(kR) J_{\ell+\frac{3}{2}}(kR) \right).\quad (22)$$

The integral over the exterior domain reads

$$\begin{aligned}\mathcal{V}_o &= \frac{1}{k_0^2 N^2 E_{\max}^2} \frac{\psi_\ell(kR)^2}{\chi_\ell(k_0 R)^2} \int_R^L \int_0^\pi \int_0^{2\pi} \chi_\ell^2(k_0 r) \|\mathbf{X}_{\ell m}(\varphi, \theta)\|^2 \sin(\theta) \, d\varphi d\theta dr \\ &= \frac{1}{N^2 k_0^2 E_{\max}^2} \frac{\psi_\ell(kR)^2}{\chi_\ell(k_0 R)^2} \left( \int_R^L \chi_\ell^2(k_0 r) \, dr \right) \left( \int_0^\pi \int_0^{2\pi} \|\mathbf{X}_{\ell m}(\varphi, \theta)\|^2 \sin(\theta) \, d\varphi d\theta \right) \\ &= \frac{\ell(\ell + 1)}{N^2 k_0 E_{\max}^2} \frac{\psi_\ell(kR)^2}{\chi_\ell(k_0 R)^2} \frac{\pi}{2} \int_R^L r Y_{\ell+\frac{1}{2}}^2(k_0 r) \, dr\end{aligned}\quad (23)$$

The last integral can be evaluated exactly thanks to [21, formula 5.54 p. 629]

$$\int x Y_p(\alpha x)^2 \, dx = \frac{x^2}{2} (Y_p(\alpha x)^2 - Y_{p-1}(\alpha x) Y_{p+1}(\alpha x)).$$

We obtain

$$\begin{aligned}
\mathcal{V}_o &= \frac{\ell(\ell+1)\pi}{4N^2 k_0 E_{\max}^2} \frac{\psi_\ell(kR)^2}{\chi_\ell(k_0 R)^2} \left( L^2 Y_{\ell+\frac{1}{2}}(k_0 L)^2 - L^2 Y_{\ell-\frac{1}{2}}(k_0 L) Y_{\ell+\frac{3}{2}}(k_0 L) \right. \\
&\quad \left. - R^2 Y_{\ell+\frac{1}{2}}(k_0 R)^2 + R^2 Y_{\ell-\frac{1}{2}}(k_0 R) Y_{\ell+\frac{3}{2}}(k_0 R) \right) \\
&= \frac{\ell(\ell+1)\pi}{4N^3 k_0 E_{\max}^2} \frac{J_{\ell+\frac{1}{2}}(kR)^2}{Y_{\ell+\frac{1}{2}}(k_0 R)^2} \left( L^2 Y_{\ell+\frac{1}{2}}(k_0 L)^2 - L^2 Y_{\ell-\frac{1}{2}}(k_0 L) Y_{\ell+\frac{3}{2}}(k_0 L) \right. \\
&\quad \left. - R^2 Y_{\ell+\frac{1}{2}}(k_0 R)^2 + R^2 Y_{\ell-\frac{1}{2}}(k_0 R) Y_{\ell+\frac{3}{2}}(k_0 R) \right). \quad (24)
\end{aligned}$$

It remains to compute  $E_{\max}$ , the maximum value of the euclidean norm of the electric field over the dielectric cavity, given by

$$E_{\max} = \sup_{r \in [0, R]} \left| \frac{\psi_\ell(kr)}{kr} \right| \times \sup_{(\theta, \varphi) \in [0, \pi] \times [0, 2\pi]} \|\mathbf{X}_{\ell m}(\theta, \varphi)\|. \quad (25)$$

We first consider the computation of the maximum of  $|\psi_\ell(kr)/kr| = |j_\ell(kr)|$ , where  $j_\ell$  denotes the spherical Bessel function of first kind, for  $r \in [0, R]$ . It is known, see e.g. [17, 18], that the global maximum of  $|j_\ell|$  coincides with the first local maximum of  $j_\ell$ . Thus, we are looking for the first zero of  $j'_\ell$  where [17, 18]

$$\forall x \in \mathbb{R} \quad j'_\ell(x) = \frac{\ell j_{\ell-1}(x) - (\ell+1) j_{\ell+1}(x)}{2\ell+1}.$$

We have  $j'_\ell(x) = 0$  if and only if

$$(\ell+1) J_{\ell+\frac{3}{2}}(x) - \ell J_{\ell-\frac{1}{2}}(x) = 0. \quad (26)$$

Thus the problem turns out to compute the first positive root of equation (26). Numerical methods for solving a nonlinear equation require either the knowledge of an interval where the root is isolated, or a first guess for this solution. An approximation based on an asymptotic expansion for the first zero (denoted  $a'_{\ell,1}$ ) of  $j'_\ell$  for large  $\ell$  is given by [18, formula 10.1.59, p. 441]

$$\begin{aligned}
a'_{\ell,1} &= (\ell + \frac{1}{2}) + 0.8086165 (\ell + \frac{1}{2})^{1/3} - 0.236680 (\ell + \frac{1}{2})^{-1/3} \\
&\quad - 0.20736 (\ell + \frac{1}{2})^{-1} + 0.0233 (\ell + \frac{1}{2})^{-5/3}. \quad (27)
\end{aligned}$$

Actually,  $a'_{\ell,1}$  can be considered as a good initial guess for the first zero of  $j'_\ell$  even for small  $\ell$ . For instance for  $\ell = 5$  we have  $a'_{\ell,1} = 6.7606$  whereas an accurate value for the first zero of  $j'_\ell$  obtained by symbolic computation is 6.7564. Thus, from a computational point of view we use the MATLAB command `fsolve` to solve (26) with an initial guess given by (27).

Next, we have to compute the maximum value of  $\|\mathbf{X}_{\ell m}(\theta, \varphi)\|$  for all  $(\theta, \varphi) \in [0, \pi] \times [0, 2\pi]$ . Since  $\mathbf{X}_{\ell m} = \nabla Y_\ell^m \wedge \mathbf{r}$ , we have

$$\|\mathbf{X}_{\ell m}(\theta, \varphi)\|^2 = C_{\ell, m}^2 \left( \frac{m^2}{\sin^2(\theta)} P_\ell^m(\cos(\theta))^2 + \sin^2(\theta) (P_\ell^m)'(\cos(\theta))^2 \right)$$

which is a quantity independent of  $\varphi$ . From the following relation for the derivative of the associated Legendre function  $P_\ell^m$  [21, formula 8.733 p. 965]

$$\forall x \in ]-1, 1[ \quad (P_\ell^m)'(x) = \frac{1}{1-x^2} \left( P_\ell^m(x) - (\ell - m + 1) P_{\ell+1}^m(x) \right)$$

we deduce that

$$\begin{aligned} \|\mathbf{X}_{\ell m}(\theta, \varphi)\|^2 = & \frac{C_{\ell, m}^2}{\sin^2(\theta)} \left( (m^2 + 1) P_\ell^m(\cos(\theta))^2 + (\ell - m + 1)^2 P_{\ell+1}^m(\cos(\theta))^2 \right. \\ & \left. - 2(\ell - m + 1) P_\ell^m(\cos(\theta)) P_{\ell+1}^m(\cos(\theta)) \right). \end{aligned} \quad (28)$$

Analytical computation of the maximum value of  $\|\mathbf{X}_{\ell m}(\theta, 0)\|^2$  for  $\theta \in [0, \pi]$  seems out of reach. Therefore, in the WGMODE toolbox we proceed by using numerical optimization methods. Unfortunately, expression (28) is not well suited for numerical computation purposes. Indeed for  $\ell$  larger than 150 the values of the associated Legendre function  $P_\ell^m$  are not anymore representable in the floating point arithmetic in MATLAB. As a consequence, we introduce the Schmidt semi-normalized associated Legendre functions  $S_\ell^m$  instead of the associated Legendre functions  $P_\ell^m$ . They are related to each other by the relation [22]

$$\forall x \in ]-1, 1[ \quad S_\ell^m(x) = \begin{cases} P_\ell(x) & \text{if } m = 0 \\ (-1)^m \sqrt{\frac{2(\ell - m)!}{(\ell + m)!}} P_\ell^m(x) & \text{if } m > 0 \end{cases} \quad (29)$$

We set  $D_{\ell, 0} = 1$  and  $D_{\ell, m} = (-1)^m \sqrt{(\ell + m)! / 2(\ell - m)!}$  for  $m > 0$  so that for all  $x \in ]-1, 1[$  we have  $P_\ell^m(x) = D_{\ell, m} S_\ell^m(x)$ . In terms of the Schmidt semi-normalized associated Legendre functions, we have

$$\begin{aligned} \|\mathbf{X}_{\ell m}(\theta, \varphi)\|^2 = & \frac{C_{\ell, m}^2 D_{\ell, m}^2}{\sin^2(\theta)} \left( (m^2 + 1) S_\ell^m(\cos(\theta))^2 + ((\ell + 1)^2 - m^2) S_{\ell+1}^m(\cos(\theta))^2 \right. \\ & \left. - 2\sqrt{(\ell + 1)^2 - m^2} S_\ell^m(\cos(\theta)) S_{\ell+1}^m(\cos(\theta)) \right) \end{aligned} \quad (30)$$

where

$$C_{\ell, m}^2 D_{\ell, m}^2 = \begin{cases} \frac{2\ell + 1}{4\pi} & \text{if } m = 0 \\ \frac{2\ell + 1}{8\pi} & \text{if } m > 0 \end{cases}.$$

In the WGMODE toolbox, the global maximum of  $\|\mathbf{X}_{\ell m}(\theta, 0)\|^2$  over  $[0, \pi]$  is computed numerically using MATLAB `fminunc` routine. A Trust Region Method algorithm is chosen which requires to provide the gradient of  $\|\mathbf{X}_{\ell m}(\theta, 0)\|^2$ . The initial guess for the optimization algorithm is obtained by comparing the values of  $\|\mathbf{X}_{\ell m}(\theta, 0)\|^2$  over a coarse subdivision of the interval  $[0, \pi]$ .

### 3.2. Volume of a TM mode

For TM modes, the magnetic induction is given by

$$\underline{\mathbf{B}}(r, \theta, \varphi) = \begin{cases} \frac{i}{\omega} \frac{\psi_\ell(kr)}{r} \mathbf{X}_{\ell m}(\theta, \varphi) & \text{if } r < R \\ \frac{i}{\omega} \frac{\psi_\ell(kR)}{\chi_\ell(k_0 R)} \frac{\chi_\ell(k_0 r)}{r} \mathbf{X}_{\ell m}(\theta, \varphi) & \text{if } r > R \end{cases} \quad (31)$$

and the integral (17) in spherical coordinates reads

$$\mathcal{V} = \frac{c^2}{N^2 E_{\max}^2} \int_0^L \int_0^\pi \int_0^{2\pi} \|\mathbf{B}(\mathbf{r})\|^2 r^2 \sin(\theta) \, d\varphi d\theta dr \quad (32)$$

where  $L$  is a positive number chosen such that the magnetic induction can be neglected at a radial distance greater than  $L$ . (This assumption is made possible from the evanescent behavior of the WGM field outside the micro-resonator.) Using Chasles's theorem, we split the integral into two parts such that the first integral holds over the cavity and the second integral holds over the exterior domain. The first integral reads

$$\mathcal{V}_i = \frac{1}{k^2 E_{\max}^2} \int_0^R \int_0^\pi \int_0^{2\pi} \psi_\ell^2(kr) \|\mathbf{X}_{\ell m}(\varphi, \theta)\|^2 \sin(\theta) \, d\varphi d\theta dr \quad (33)$$

and we recognize the same integral as in (20). Therefore, we directly deduce that

$$\mathcal{V}_i = \frac{\ell(\ell+1)\pi R^2}{4k E_{\max}^2} \left( J_{\ell+\frac{1}{2}}(kR)^2 - J_{\ell-\frac{1}{2}}(kR)J_{\ell+\frac{3}{2}}(kR) \right). \quad (34)$$

The integral over the exterior domain reads

$$\begin{aligned} \mathcal{V}_o &= \frac{1}{k^2 E_{\max}^2} \int_R^L \int_0^\pi \int_0^{2\pi} \|\mathbf{B}(r, \theta, \varphi)\|^2 \sin(\theta) \, d\varphi d\theta dr \\ &= \frac{1}{k^2 E_{\max}^2} \frac{\psi_\ell(kR)}{\chi_\ell(k_0 R)} \int_R^L \int_0^\pi \int_0^{2\pi} \chi_\ell^2(k_0 r) \|\mathbf{X}_{\ell m}(\varphi, \theta)\|^2 \sin(\theta) \, d\varphi d\theta dr. \end{aligned} \quad (35)$$

Once again, the integral has already been computed, see (23). Therefore, we immediately obtain

$$\begin{aligned} \mathcal{V}_o &= \frac{\ell(\ell+1)\pi}{4k E_{\max}^2} \frac{J_{\ell+\frac{1}{2}}(kR)^2}{Y_{\ell+\frac{1}{2}}(k_0 R)^2} \left( L^2 Y_{\ell+\frac{1}{2}}(k_0 L)^2 - L^2 Y_{\ell-\frac{1}{2}}(k_0 L) Y_{\ell+\frac{3}{2}}(k_0 L) \right. \\ &\quad \left. - R^2 Y_{\ell+\frac{1}{2}}(k_0 R)^2 + R^2 Y_{\ell-\frac{1}{2}}(k_0 R) Y_{\ell+\frac{3}{2}}(k_0 R) \right). \end{aligned} \quad (36)$$

It remains to compute  $E_{\max}^2$  the maximum value of the euclidean norm of the electric field. Since the electromagnetic field for a WGM is at its peak inside

the cavity, we deduce from (9) that

$$E_{\max}^2(r, \theta) = \frac{C_{\ell, m}^2}{k^2 r^2} \left( \ell^2 (\ell + 1)^2 \frac{|\psi_\ell(kr)|^2}{k^2 r^2} P_\ell^m(\cos \theta)^2 + |\psi'_\ell(kr)|^2 \left( (\sin(\theta)(P_\ell^m)'(\cos \theta))^2 + \left( \frac{m}{\sin(\theta)} P_\ell^m(\cos \theta) \right)^2 \right) \right). \quad (37)$$

Analytical computation of the maximum value of  $E_{\max}^2$  over  $[0, R] \times [0, \pi]$  is out of reach. Therefore, in the WGMODE toolbox we proceed by using numerical optimization methods and to this purpose, we express  $E_{\max}^2$  in terms of Schmidt semi-normalized associated Legendre functions  $S_\ell^m$  and Bessel's functions:

$$E_{\max}^2(r, \theta) = \frac{C_{\ell, m}^2 D_{\ell, m}^2}{k^2 r^2} \frac{\pi}{2} \left( \ell^2 (\ell + 1)^2 \frac{|J_{\ell + \frac{1}{2}}(kr)|^2}{kr} S_\ell^m(\cos \theta)^2 + \left| (kr)^{\frac{1}{2}} J_{\ell - \frac{1}{2}}(kr) - \ell (kr)^{-\frac{1}{2}} J_{\ell + \frac{1}{2}}(kr) \right|^2 \left( (m^2 + 1) S_\ell^m(\cos \theta)^2 - 2\sqrt{(\ell + 1)^2 - m^2} S_\ell^m(\cos \theta) S_{\ell + 1}^m(\cos \theta) + ((\ell + 1)^2 - m^2) S_{\ell + 1}^m(\cos \theta)^2 \right) \right). \quad (38)$$

In order to compute the global maximum of  $E_{\max}^2$  over  $[0, R] \times [0, \pi]$  we use MATLAB `fminunc` routine designed to find minimum of unconstrained multi-variable functions. Namely, a Trust Region Method algorithm is chosen which requires to provide the gradient of  $E_{\max}^2$ . The initial guess for the optimization algorithm is obtained by comparing the values of  $E_{\max}^2$  over a coarse grid of the domain  $[0, R] \times [0, \pi]$ .

## 4. Overview of the Matlab Toolbox WGMmode

### 4.1. Numerical issues addressed in the WGMODE toolbox

Computation of WGM in a spherical optical micro-resonator must address the following issue. Resonance wavelengths (corresponding to the visible spectrum) are obtained by solving the modal equation (11) that relies on the polar mode index  $\ell \in \mathbb{N}$ . If one sets any value for the integer  $\ell$ , there is a strong possibility that the solutions to the modal equation (11) (if they exist) do not correspond to wavelengths in the visible spectrum and even fewer to WGM. In practice, one is interested by WGM around a given wavelength, say  $\lambda \approx 1.5 \mu\text{m}$ . However, if one sets the value of  $\lambda$  and solves the modal equation (11) for the polar mode index  $\ell$  there will be little chance that the value of  $\ell$  will be an integer. To overcome this issue, we have to proceed in two steps.

1. In a first step, we set the value of the wavelength  $\lambda$  corresponding to a rough approximation of the wavelength of the WGM sought after and we solve the modal equation for the polar mode index  $\ell$ . We obtain a set of solutions that are not integer.

2. In a second step, we choose one of the solutions (say the highest for the fundamental mode) and we round it to the nearest integer. We solve once again the modal equation with this integer value of  $\ell$  to determine the resonance wavelengths. Because of the continuity of the solutions to the modal equation with respect to the equation's parameters, the first solution (corresponding to a radial mode index  $n = 1$ ) will be close to the target value.

Another important issue lies in the solving of the modal equation (11). Indeed, because Riccati-Bessel function of the third kind (just as Hankel's functions) is complex valued, solutions to the modal equation (11) are complex numbers (the imaginary part of which takes into account losses and is required to compute the Q-factor). From a numerical point of view, it is much more difficult to solve a non-linear equation in the complex plane than in the real line. Therefore, we proceed in two steps. We first solve the approximated modal equation (14) on the real line. Then, each real solution of the approximated modal equation (14) is used as an initial guess for the iterative method implemented in the MATLAB `fsolve` routine to solve the modal equation (11).

For numerical purposes it is more convenient to express the modal equation (14) in terms of Bessel functions of first and second kind. We obtain

$$\frac{Y_{\ell-\frac{1}{2}}(k_0R)}{Y_{\ell+\frac{1}{2}}(k_0R)} - P \frac{J_{\ell-\frac{1}{2}}(kR)}{J_{\ell+\frac{1}{2}}(kR)} = \ell \left( \frac{1}{k_0R} - \frac{P}{kR} \right). \quad (39)$$

For a given mode number  $\ell$ , the wavelengths  $\lambda$  for which resonance occurs are obtained by solving equation (39), that is to say by looking for the zeros of the modal function

$$F_\ell : \lambda \in ]0, +\infty[ \mapsto \frac{Y_{\ell-\frac{1}{2}}(k_0R)}{Y_{\ell+\frac{1}{2}}(k_0R)} - P \frac{J_{\ell-\frac{1}{2}}(kR)}{J_{\ell+\frac{1}{2}}(kR)} - \ell \left( \frac{1}{k_0R} - \frac{P}{kR} \right). \quad (40)$$

In the WGMODE toolbox, the zeros of this non-linear function on the real line are computed thanks to MATLAB's `fzero` function. It is very useful from a practical point of view to use the following bounds for the solutions corresponding to WGM provided in [9, p. 25]. For a given  $\lambda$ , the mode numbers  $\ell$  corresponding to solutions to the modal equation (14) are such that

$$\frac{2\pi(R + \delta_P)}{\lambda} < \ell + \frac{1}{2} < N \frac{2\pi(R + \delta_P)}{\lambda} \quad (41)$$

where  $\delta_P \approx \frac{\lambda}{2\pi N} \frac{P}{\sqrt{N^2-1}}$ . There is no solution  $\ell$  to (14) greater than the upper bound value in (41). Conversely, there are some solutions lower than the lower bound value, but they do not correspond to WGM. Relation (41) implies that for a fixed value of  $\ell$  the wavelengths  $\lambda$  for which resonance occurs are such that

$$\frac{2\pi R}{\ell + \frac{1}{2} - \alpha} < \lambda < \frac{2\pi RN}{\ell + \frac{1}{2} - \alpha N} \quad (42)$$

where  $\alpha = P/(N\sqrt{N^2 - 1})$ . The WGMODE toolbox uses relations (41) and (42) in the root finding process but one can easily ignore these bounds and provide its own bounds by setting the `expert_mode` variable to the value 1 in the main program. In order to be sure to compute all the solutions to the approximated modal equation (14), the interval defined by the above lower and upper bounds is discretized with a very small step-size and sign changes in the values taken by the non-linear function (40) are detected. Then, MATLAB's `fzero` routine is used to accurately compute each solution in the interval it has been located.

To compute the quality factor, one has to solve the exact modal equation (11) in the complex plane. This is achieved by using MATLAB's `fsolve` routine with an initial guess for the iterative algorithm used in `fsolve` given by the (real) solution obtained by solving the approximated modal equation (14) modified by adding a very small imaginary part (MATLAB documentation recommends to set a complex initial point when using the non-linear equation solver `fsolve` in the complex plane). This approach is implemented in the script `qfact.m` of the WGMODE toolbox. Alternatively, since solving the modal equation (11) amounts to locate the zeros of an analytical function, this can be achieved by computing by quadrature contour integrals in the complex plane according to the Delves-Lyness Method [23, 24]. This approach is implemented in the script `qfactn.m` of the WGMODE toolbox.

We would like to draw attention to the fact that the solutions to the modal equation (11) are complex numbers with a very small imaginary part compared to its real part and that solving equation (11) represents a stiff problem from a numerical point of view. The user should pay attention to the information returned by MATLAB `fsolve` routine used to solve equation (11) to decide on the reliability of the radiative quality factor value. Moreover, even if computed accurately, this value can differ significantly from the experimentally measured quality factor because of intrinsic loss sources not taken into account in the radiative quality factor but that can be predominant compared to radiative losses.

Particular attention has been paid to the numerical computation of  $E_{\max}^2$  the maximum value of the euclidean norm of the electric field by optimization methods. Since optimization methods such as the ones implemented in MATLAB `fminunc` routine can't make a distinction between local maxima and the global maximum and because in general convergence is only ensured when the initial guess is sufficiently close to the global maximum, we first have to compute a reliable initial guess. To this purpose, we compare the values of  $E_{\max}^2$  over a coarse grid of the optimization domain (the interval  $[0, \pi]$  for TE modes or the set  $[0, R] \times [0, \pi]$  for TM modes). Then, the global maximum of  $E_{\max}^2$  is computed by using the `fminunc` routine for unconstrained optimization problem where a Trust Region algorithm is chosen. The Trust Region method requires that the gradient of  $E_{\max}^2$  is provided. Since the `fminunc` routine could sometimes converge to a local maximum, we compare the maximum provided by `fminunc` to the value of the objective function with the initial guess. If the two values differ too much, we consider more reliable and safe to use a brute force method to compute the global maximum that consists in comparing the values of  $E_{\max}^2$  over

a very fine grid of the optimization domain. Finally, to overcome the possible absence of the optimization toolbox in the user MATLAB installation, we test if the toolbox is available and if this is not so, we use the above mentioned brute force method to compute the global maximum.

#### 4.2. WGMODE toolbox contents

The WGMODE toolbox is constituted of various MATLAB scripts aimed at studying WGM in spherical optical micro-resonators. They allow to explore resonance conditions for TE or TM modes, to visualize WGM in a micro-sphere and to compute the volume and quality factor of any given mode. Namely, the WGMODE toolbox contains the following MATLAB scripts:

- ELLRES computes, for a given wavelength, the values of the mode index  $\ell$  for which a resonance occurs (note that the solutions  $\ell$  are real numbers);
- WVLRES computes, for a given polar mode index  $\ell$  the values of the wavelength for which a resonance occurs;
- VOLMOD computes the volume of a whispering gallery mode in a micro-sphere;
- QFACT computes for a given whispering gallery mode its quality factor by solving the modal equation by `fsolve`;
- QFACTN computes for a given whispering gallery mode its quality factor by solving the modal equation by the Delves-Lyness Method;
- PLTMOD plots a whispering gallery mode.

The general organization of the WGMODE toolbox is depicted in Fig. 2. The toolbox also provides a collection of special functions:

- SLEGEND associated Legendre function with Schmidt semi-normalization;
- SBESSELJ spherical Bessel function of the first kind;
- SBESSELY spherical Bessel function of the second kind;
- SBESSELH spherical Bessel function of the third kind (Hankel function);
- DSLEGEND derivative of the associated Legendre function with Schmidt semi-normalization;
- DSBESSELJ derivative of the spherical Bessel function of the first kind;
- DSBESSELY derivative of the spherical Bessel function of the second kind;
- DSBESSELH derivative of the spherical Bessel function of the third kind (Hankel function);
- HANSENM Hansen solution  $\mathbf{M}_\ell^m$  of the spherical vectorial wave equation;

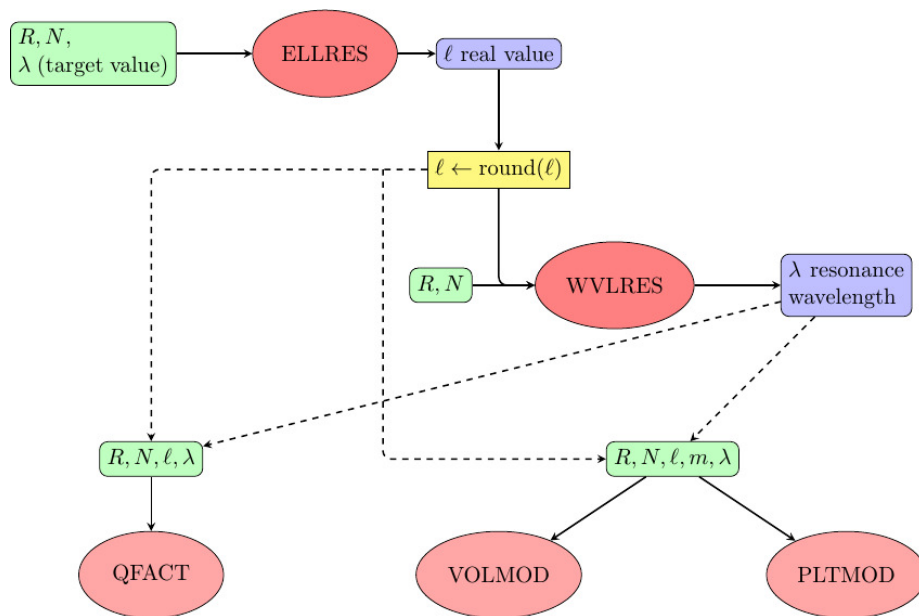


Figure 2: General organization of the WGMODE toolbox.  $R$  denotes the sphere radius,  $N$  its optical index.  $\lambda$  is the resonance wavelength of the mode and  $\ell, m$  its indexes. The scripts ELLRES and WVLRES are used to compute the resonant mode features around a wavelength target value. The scripts QFACT, VOLMOD can be used to compute key attributes of the mode. PLTMOD allows to display the mode.

- HANSENN Hansen solution  $\mathbf{N}_\ell^m$  of the spherical vectorial wave equation.

Lastly, the WGMODE toolbox contains low level internal functions:

- MODEQEL Modal equation (14) for TE or TM modes for a fixed wavelength and a variable mode index;
- MODEQWV Modal equation (14) for TE or TM modes for a fixed mode index  $\ell$  and a variable wavelength;
- CMODEQWV Modal equation (11) for TE or TM modes for a fixed mode index  $\ell$  and a variable wavelength;
- PLOTD plots a discontinuous function removing the draw line at function discontinuity jumps;
- VSHNOR computes the square of the euclidean norm of the vector spherical harmonics;
- FOPTE/FOPTM objective function (and its gradient) required to compute the maximum of the square of the euclidean norm of the electric field for TE/TM modes;
- MODEFIELD computes the electromagnetic field (electric field and magnetic induction) of a given mode;
- INTGDL integrand in the Delves-Lyness Method used to solve the modal equation in the complex plane.

#### 4.3. A comprehensive test run

In order to illustrate the use of the WGMODE toolbox, we consider a micro-sphere of radius  $50 \mu\text{m}$  and optical index 1.5, see [5]. We are interested in resonance conditions around a wavelength of 1500 nm. First, we use the script entitled `ellres` to determine the solutions  $\ell$  to the approximated modal equation (14) for wave numbers  $k$  and  $k_0$  corresponding to a wavelength of 1500 nm and to a TE mode.

```
>> ellres
Micro-sphere radius [micro-m] = 50
Optical index of the micro-sphere = 1.5
TE or TM mode ? (TE/TM) : TE
Wavelength [nm] = 1500

Polar mode indexes ell:

| 1 | 302.418 |      | 7 | 261.233 |      | 13 | 233.160 |
| 2 | 293.024 |      | 8 | 256.086 |      | 14 | 228.991 |
| 3 | 285.350 |      | 9 | 251.163 |      | 15 | 224.932 |
| 4 | 278.578 |      | 10 | 246.432 |      | 16 | 220.977 |
| 5 | 272.399 |      | 11 | 241.867 |      | 17 | 217.125 |
| 6 | 266.649 |      | 12 | 237.448 |      | 18 | 213.356 |
```

Note that an expert mode can be activated by setting the variable `expert_mode` to 1 in the `ellres` program. It provides a plot of the modal function  $F_\lambda : \ell \in ]0, +\infty[ \mapsto \frac{Y_{\ell-\frac{1}{2}}(k_0 R)}{Y_{\ell+\frac{1}{2}}(k_0 R)} - P \frac{J_{\ell-\frac{1}{2}}(kR)}{J_{\ell+\frac{1}{2}}(kR)} - \ell \left( \frac{1}{k_0 R} - \frac{P}{kR} \right)$ , the zero of which are the sought out solutions.

As it can be seen above, the polar mode indexes  $\ell$  obtained as solutions to the modal equation (11) are not integers. Thus, we have to round up the values to the nearest integer. But by doing so, the couple  $(\lambda, \ell)$  does not anymore satisfy the modal equation. For each rounded value for  $\ell$ , we have to compute the resonance wavelength by solving once again the modal equation. This time,  $\ell$  is fixed and we look for  $\lambda$ . Computation is achieved with the MATLAB script `wlres`. As an example, we consider the first value for  $\ell$  (302.418), rounded to 302.

```
>> wlres
Micro-sphere radius [micro-m] = 50
Optical index of the micro-sphere = 1.5
TE or TM mode ? (TE/TM) : TE
Mode index ell = 302

Wavelength interval of interest found [nm] = [1041.6229 , 1564.7545]

Radial mode number and resonance wavelength [nm]:

| 1 | 1502.024424 | | 10 | 1260.273611 | | 19 | 1128.758252 |
| 2 | 1457.369250 | | 11 | 1242.923923 | | 20 | 1116.755046 |
| 3 | 1422.192876 | | 12 | 1226.431024 | | 21 | 1105.138953 |
| 4 | 1392.096286 | | 13 | 1210.700903 | | 22 | 1093.888044 |
| 5 | 1365.368812 | | 14 | 1195.656160 | | 23 | 1082.984747 |
| 6 | 1341.115707 | | 15 | 1181.232108 | | 24 | 1072.412699 |
| 7 | 1318.793286 | | 16 | 1167.373999 | | 25 | 1062.143903 |
| 8 | 1298.039229 | | 17 | 1154.035012 | | 26 | 1052.121851 |
| 9 | 1278.596368 | | 18 | 1141.174768 | | 27 | 1042.266580 |
```

An expert mode can be activated by setting the variable `expert_mode` to 1 in the `wlres` program. It allows to compare the resonance wavelengths to the one obtained from the Eikonale approach, see e.g. [5, 9], which basically relies on asymptotic expansion for Bessel's functions of large order. It also provides a plot of the modal function  $F_\ell$  defined in (40).

It is possible thanks to the `pltmod` script in the `WGMODE` toolbox to draw the WGM field. Three different plots of the euclidean norm of the electric field  $\|\underline{\mathbf{E}}(r, \theta, \varphi)\|$  and magnetic induction  $\|\underline{\mathbf{B}}(r, \theta, \varphi)\|$  are proposed. They correspond to a 1D-plot in the radial direction, to a 2D-plot in an azimuthal plane  $\varphi = \text{cste}$  and to a 2D-plot in a polar plane  $\theta = \text{cste}$ . We have depicted in Fig. 3 the radial variation of the electric field and magnetic induction for  $(\theta, \varphi) = (\frac{\pi}{2}, 0)$  corresponding to the TE mode with polar index  $\ell = 302$  and radial index  $n = 5$ .

It has a resonance wavelength of 1365.36812 nm. Note that the unit is arbitrary since the mode field is defined up to a multiplicative constant. One can clearly see the five expected maxima in the radial direction for a mode with radial index  $n = 5$ . One can also see that both the electric field and magnetic induction are continuous across the sphere border as expected for TE modes. This would not be the case for a TM mode.

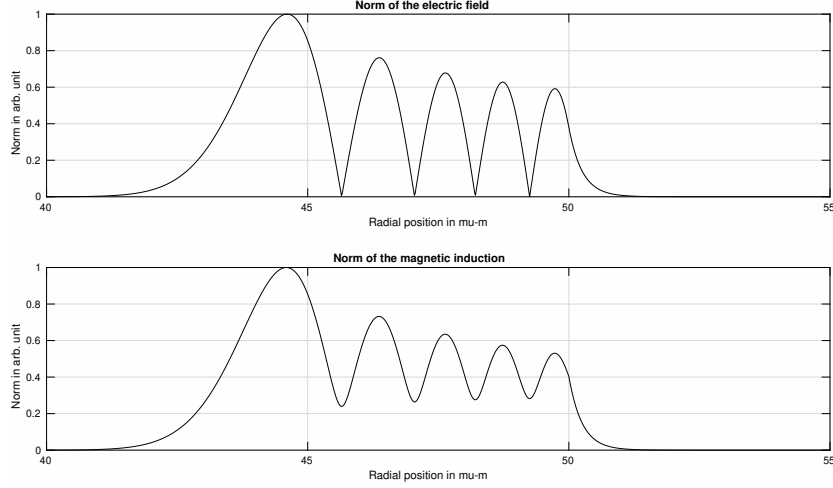


Figure 3: Radial behavior of the TE mode with polar index  $\ell = 302$  and radial index  $n = 5$  of a micro-sphere with radius  $R = 50 \mu\text{m}$  and optical index  $N = 1.5$ .

The `pltmod` script also allows to draw the WGM field in an azimuthal plane  $\varphi = \text{cste}$  as shown in Fig. 4 where we have represented the euclidean norm of the electric field and magnetic induction in the plane  $\varphi = 0$  for the WGM with indexes  $\ell = 302, m = 300, n = 1$  ( $\lambda = 1502.024 \text{ nm}$ ) in the case of a spherical cavity with radius  $R = 50 \mu\text{m}$  and optical index  $N = 1.5$ . Note that the norm of the electric field (resp. magnetic induction) is given in arbitrarily units since the WGM field is defined up to a multiplicative constant. Since a zoom in the area of interest in the MATLAB graphical window induces a loss in the image rendering, an expert mode is provided in the `pltmod` script (obtained by turning the variable `expert_mode` to the value 1 in the script). When this option is chosen it is possible to indicate the bounds of the area to plot (bounds for the polar angle  $\theta$  and radial distance  $r$ ). Fig. 4 was obtained using this feature with the following bounds:  $r \in [0.8 R, 1.1 R]$  and  $\theta \in [0.8 \frac{\pi}{2}, 1.2 \frac{\pi}{2}]$ . One can see in Fig. 4 that for the chosen data, we have  $\ell - |m| + 1 = 3$  which is the number of intensity maxima in the polar direction  $\mathbf{e}_\theta$  as stated on p. 6. Similarly, it is possible with the `pltmod` script to draw the WGM field in an azimuthal plane  $\theta = \text{cste}$ .

With all the information at hand, we are now in position to compute the mode volume. For the dielectric micro-sphere with radius  $R = 50 \mu\text{m}$  and optical

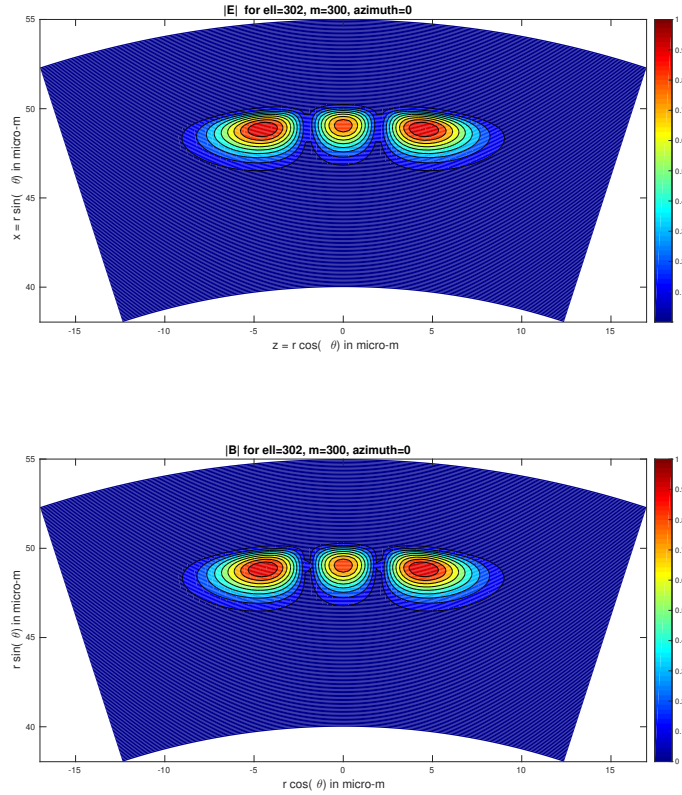


Figure 4: Euclidean norms of the electric field and magnetic induction in the plane  $\varphi = 0$  for the WGM with indexes  $\ell = 302, m = 300, n = 1$  in the case of a spherical cavity with radius  $R = 50 \mu\text{m}$  and optical index  $N = 1.5$ .

index  $N = 1.5$ , let us consider the WGM characterized by the mode indexes  $\ell = 302, m = \ell$  and  $n = 1$  for which the resonance wavelength has been found to be  $\lambda = 1502.024424 \text{ nm}$ . Thanks to the `volmod` script in the `WGMODE` toolbox, we find that the volume of this WGM is  $2259.6416 \mu\text{m}^3$  as detailed below.

```
>> volmod
Micro-sphere radius [micro-m] = 50
Optical index of the micro-sphere = 1.5
TE or TM mode ? (TE/TM) : TE
Wavelength [nm] = 1502.0244
Mode number ell = 302
Mode number m = 302
```

```
-----  
Local minimum possible.
```

```
fminunc stopped because the size of the current step is less than  
the default value of the step size tolerance.
```

```
<stopping criteria details>
```

```
-----  
Mode volume (in micron.m^3)= 2259.6416  
CPU time for mode volume computations = 1.58 sec.
```

Always for this particular WGM, using the `qfact` script, the quality factor is found to be  $1.578 \cdot 10^{17}$ . Note that this quality factor is not in accordance with the quality factor usually observed experimentally because radiative losses are much lower than intrinsic losses for such a micro-resonator. The tolerance values used to end iterations in the `fsolve` routine are set by default to  $10^{-9}$ . These tolerance values can be modified using the expert mode by setting the `expert_mode` variable to the value 1 in the `qfact` script. Because solving equation (11) represents a stiff problem from a numerical point of view, the user should pay attention to the information returned by MATLAB `fsolve` routine to decide on the reliability of the quality factor value.

```
>> qfact  
Micro-sphere radius [micro-m] = 50  
Optical index of the micro-sphere = 1.5  
TE or TM mode ? (TE/TM) : TE  
Mode index ell = 302  
Approximated real value of the resonance wavelength [nm] = 1502  
-----  
Non-linear solver fsolve informations  
  
Equation solved.  
  
fsolve completed because the vector of function values is near zero  
as measured by the selected value of the function tolerance, and  
the problem appears regular as measured by the gradient.  
  
<stopping criteria details>  
  
-----  
Complex resonance wavelength for the mode in [nm] = 1502.024424398681  
-9.518987898596565e-15i  
Quality factor for the mode = 1.578e+17
```

One should note that the ratio of the imaginary part and the real part

of the resonance is lower than the floating point accuracy and therefore the value returned for the quality factor should be considered with caution. When comparing to the result returned by the Delves-Lyness method, see below, we obtain a very good agreement for the real part of the resonance wavelength but significantly different results for the imaginary part.

```
>> qfactn
Micro-sphere radius [micro-m] = 50
Optical index of the micro-sphere = 1.5
TE or TM mode ? (TE/TM) : TE
Mode index ell = 302
Approximated real value of the resonance wavelength [nm] = 1502

One root (wavelength resonance) of the modal equation located in the disk
centered at 1502 nm with radius 1 nm

Complex resonance wavelength for the mode in [nm] = 1502.024424398681
-2.593625978591534e-17i
Quality factor for the mode = 5.791e+19
```

## 5. Numerical validation

We have compared our computational method for mode volume  $\mathcal{V}$  in spherical optical micro-resonators to the values obtained when using the Finite Elements Method (FEM) and to the values provided by the following formula [9] based on asymptotic approximation of the WGM field

$$\mathcal{V} \approx 2\pi^{\frac{3}{2}} \left( \frac{\lambda}{2\pi N} \right)^3 \frac{z_1^3}{2\sqrt{\ell}} \left( \frac{j'_\ell(z_1)}{j_\ell(z_1)} \right)^2 \quad (43)$$

where  $j_\ell$  denotes the spherical Bessel function of the first kind with order  $\ell$ ,  $z_1$  its first zero and  $z'_1$  the first zero of  $j'_\ell$ . This formula is valid for the mode volume of WGM with indexes such that  $\ell = |m|$  and  $n = 1$ . We refer to [15] for presentation of the way the mode volume of WGM can be computed by the Finite Element method. To perform the computations, we have used the open-source Finite Element software FreeFem++ [25]. We have taken into account the axial symmetry of the micro-sphere to reduce the problem to a vectorial formulation for the magnetic field set in a cylindrical two-dimensional section as explained in [15]. Computations were achieved with MATLAB 9.0 on an Intel Core i5 desktop computer (4 Cores, 4 Threads @2.50 GHz) with 8 Go memory.

We first consider the case of the micro-sphere of radius  $50 \mu\text{m}$  and optical index 1.5 discussed in section 4. Using the WGMODE toolbox, we found that the TE mode with indexes  $\ell = m = 302, n = 1$  has a resonance wavelength  $\lambda = 1502.0244 \text{ nm}$  and a volume  $\mathcal{V} = 2259.64 \mu\text{m}^3$ . Computation of the mode volume took 1.5 sec. Using the approximated formula (43), we obtain a mode volume

of  $2258.76 \mu\text{m}^3$ . The values provided by the FEM are a resonance wavelength of  $1502.0195 \text{ nm}$  and a mode volume of  $2259.79 \mu\text{m}^3$ . The FEM computation with Lagrange  $P_3$  Finite Elements and 30474 mesh elements took 324.89 sec. Note that the FEM can compute several modes at once (10 in our simulation) with a low over-cost. The relative difference on the mode volume computed by the FEM and the WGMODE toolbox is  $6.6 \cdot 10^{-5}$ .

When considering the TM mode with the same indexes  $\ell = m = 302, n = 1$ , we found a resonance wavelength  $\lambda = 1498.4979 \text{ nm}$  and volume  $\mathcal{V} = 2334.89 \mu\text{m}^3$  with the WGMODE toolbox. Computation of the mode volume took 4.4 sec. Compared to the computation of the TE mode volume, this higher computation time is explained by the computation of the maximum value of the electric field that is more complicated for TM modes, see Section 3.2. For TM modes the only comparison is with the FEM. The FEM provided a resonance wavelength  $\lambda = 1498.4923 \text{ nm}$  and a mode volume  $\mathcal{V} = 2335.59 \mu\text{m}^3$ . The relative difference between the mode volume given by the two methods is  $3.0 \cdot 10^{-4}$ .

As a second benchmark test, we consider a micro-sphere with radius  $25 \mu\text{m}$  and optical index 1.453 and the TE mode with indexes  $\ell = 271, m = 271$ . The mode volume obtained by formula (43) is  $319.03 \mu\text{m}^3$ . Using the WGMODE toolbox we found a resonance wavelength of  $808.6104 \text{ nm}$  and a mode volume of  $319.21 \mu\text{m}^3$ . The values provided by the FEM are a resonance wavelength of  $808.6073 \text{ nm}$  and a mode volume of  $319.30 \mu\text{m}^3$ . The FEM computation with Lagrange  $P_3$  Finite Elements and 25998 mesh elements took 131.7 sec. (10 modes are computed at the same time) whereas using the WGMODE toolbox, the mode volume was computed in 1.6 sec. The relative difference between the mode volume given by the two methods is  $2.8 \cdot 10^{-4}$ .

As a last benchmark test, we consider a micro-sphere with radius  $25 \mu\text{m}$  and optical index 1.453 and the TM mode with indexes  $\ell = 271, m = 270$  and  $n = 2$ . Formula (43) can not be used for such modal index values. Using the WGMODE toolbox we found a resonance wavelength of  $780.9564 \text{ nm}$  and for the mode volume  $542.83 \mu\text{m}^3$ . The computation took 4 sec. The values provided by the FEM are a resonance wavelength of  $780.9533 \text{ nm}$  and a mode volume of  $539.88 \mu\text{m}^3$ . The computation with Lagrange  $P_3$  Finite Elements and 25998 mesh elements took 262.0 sec. (10 modes are computed at the same time). The relative difference between the mode volume given by the two methods is  $5.3 \cdot 10^{-3}$ .

## 6. Conclusion

We have presented a MATLAB toolbox aimed at studying whispering gallery modes (WGM) in spherical optical micro-resonators. Its originality comes from analytical formulas used to compute the volume of WGM which provide fast and accurate results. Such a software development has been made possible because of the existence of analytical expressions for the electromagnetic field of a WGM in a spherical dielectric cavity and the existence of exact quadrature formulas for various integrands involving Bessel's functions in the literature. It would be difficult to extend the toolbox to other geometries of the dielectric cavity.

However, a future development of the WGMODE toolbox could be envisaged to cover optical micro-bubble resonators [13].

## Acknowledgments

The author would like to thank Patrice Féron, from Foton Laboratory, ENSSAT-University of Rennes 1, for the numerous discussions on optical micro-resonators and for his constant support.

## References

- [1] A. B. Matsko, V. S. Ilchenko, Optical resonators with whispering-gallery modes-part I: Basics, *IEEE Journal of Selected Topics in Quantum Electronics* 12 (1) (2006) 3–14. doi:10.1109/JSTQE.2005.862952.
- [2] A. Chiasera, Y. Dumeige, P. Féron, M. Ferrari, Y. Jestin, G. Nunzi-Conti, S. Pelli, S. Soria, G. Righini, Spherical whispering-gallery-mode microresonators, *Laser and Photonics Reviews* 4 (3) (2010) 457–482. doi:10.1002/lpor.200910016.
- [3] T. Benson, S. Boriskina, P. Sewell, A. Vukovic, S. Greedy, A. Nosich, *Frontiers in Planar Lightwave Circuit Technology*. NATO Science Series II: Mathematics, Physics and Chemistry, Springer, Dordrecht, 2006, Ch. Micro-optical resonators for microlasers and integrated optoelectronics.
- [4] J. Ward, O. Benson, WGM microresonators: sensing, lasing and fundamental optics with microspheres, *Laser & Photonics Reviews* 5 (4) (2011) 553–570. doi:10.1002/lpor.201000025.
- [5] G. C. Righini, Y. Dumeige, P. Féron, M. Ferrari, G. N. Conti, D. Ristic, S. Soria, Whispering gallery mode microresonators: Fundamentals and applications, *Rivista del Nuovo Cimento* 34 (7) (2011) 435–488. doi:10.1393/ncr/i2011-10067-2.
- [6] R. Talebi, K. Abbasian, A. Rostami, Analytical modeling of quality factor for shell type microsphere resonators, *Progress In Electromagnetics Research B* 30 (2011) 293–311. doi:10.2528/PIERB11040303.
- [7] M. Borselli, T. Johnson, O. Painter, Beyond the Rayleigh scattering limit in high-Q silicon microdisks: Theory and experiment, *Opt. Express* 13 (5) (2005) 1515–1530. doi:10.1364/OPEX.13.001515.
- [8] A. N. Oraevsky, Review: Whispering-gallery waves, *Quantum Electronics* 32 (2002) 377–400. doi:10.1070/QE2002v032n05ABEH002205.
- [9] F. Treussart, Étude expérimentale de l’effet laser dans des micro-sphères de silice dopées avec des ions néodyme, Ph.D. thesis, Université Pierre et Marie Curie, Paris, France (1997).

- [10] T.J.A.Kippenberg, Nonlinear optics in ultra-high-Q whispering-gallery optical microcavities, Ph.D. thesis, California Institute of Technology, Pasadena, California, USA (2004).
- [11] E. A. Muljarov, W. Langbein, Exact mode volume and Purcell factor of open optical systems, *Phys. Rev. B* 94 (2016) 235438. doi:10.1103/PhysRevB.94.235438.
- [12] X. Wu, Y. Wang, Q. Chen, Y.-C. Chen, X. Li, L. Tong, X. Fan, High-q, low-mode-volume microsphere-integrated fabry-perot cavity for optofluidic lasing applications, *Photon. Res.* 7 (1) (2019) 50–60. doi:10.1364/PRJ.7.000050.
- [13] A. Barucci, S. Berneschi, A. Giannetti, F. Baldini, A. Cosci, S. Pelli, D. Farnesi, G. C. Righini, S. Soria, G. Nunzi Conti, Optical microbubble resonators with high refractive index inner coating for bio-sensing applications: An analytical approach, *Sensors* 16 (12). doi:10.3390/s16121992.
- [14] K. Srinivasan, M. Borselli, O. Painter, A. Stintz, S. Krishna, Cavity Q, mode volume, and lasing threshold in small diameter AlGaAs microdisks with embedded quantum dots, *Opt. Express* 14 (3) (2006) 1094–1105. doi:10.1364/OE.14.001094.
- [15] M. Oxborrow, Traceable 2-D Finite-Element simulation of the whispering-gallery modes of axisymmetric electromagnetic resonators, *IEEE Transactions on Microwave Theory and Techniques* 55 (6) (2007) 1209–1218. doi:10.1109/TMTT.2007.897850.
- [16] J. Stratton, *Electromagnetic Theory*, Wiley, 2007.
- [17] F. Olver, D. Lozier, R. Boisvert, C. Clark, *NIST Handbook of Mathematical Functions*, Cambridge University Press, 2010.
- [18] M. Abramowitz, I. A. Stegun, *Handbook of Mathematical Functions: with Formulas, Graphs, and Mathematical Tables*, Dover Publications, 1965.
- [19] K. Atkinson, W. Han, *Spherical Harmonics and Approximations on the Unit Sphere: An Introduction*, *Lecture Notes in Mathematics*, Springer, 2012.
- [20] J. D. Jackson, *Classical Electrodynamics*, 3rd Edition, Wiley, 1998.
- [21] I. S. Gradshteyn, I. M. Ryzhik, *Table of Integrals, Series, and Products*, Elsevier Science, 2007.
- [22] D. E. Winch, D. J. Ivers, J. P. R. Turner, R. J. Stening, Geomagnetism and Schmidt quasi-normalization, *Geophysical Journal International* 160 (2) (2005) 487–504. doi:10.1111/j.1365-246X.2004.02472.x.
- [23] L. M. Delves, J. N. Lyness, A numerical method for locating the zeros of an analytic function, *Math. Comp.* 21 (1967) 543–560. doi:10.2307/2004999.

- [24] N. I. Ioakimidis, Quadrature methods for the determination of zeros of transcendental functions - a review, in: P. Keast, G. Fairweather (Eds.), Numerical Integration: Recent Developments, Software and Applications, Springer Netherlands, Dordrecht, 1987, pp. 61–82. doi:10.1007/978-94-009-3889-2\_5.
- [25] F. Hecht, New development in FreeFem++, J. Numer. Math. 20 (3-4) (2012) 251–265. doi:10.1515/jnum-2012-0013.